

# The Phosphoinositide Kinase PIKfyve/Fab1p Regulates Terminal Lysosome Maturation in *Caenorhabditis elegans*

Anne-Sophie Nicot,\* Hanna Fares,<sup>†</sup> Bernard Payraastre,<sup>‡</sup> Andrew D. Chisholm,<sup>§</sup> Michel Labouesse,<sup>||</sup> and Jocelyn Laporte\*

Departments of \*Molecular Pathology and <sup>||</sup>Developmental Biology, Institut de Génétique et de Biologie Moléculaire et Cellulaire, Institut National de la Santé et de la Recherche Médicale U596, Centre National de la Recherche Scientifique Unité Mixte de Recherche 7104, Université Louis Pasteur de Strasbourg, Collège de France, 67404 Illkirch, France; <sup>†</sup>Department of Molecular and Cellular Biology, University of Arizona, Tucson, AZ 85721; <sup>‡</sup>Oncogenesis and Signaling in Hematopoietic Cells, Institut National de la Santé et de la Recherche Médicale U563, Centre de Physiopathologie de Toulouse Purpan, Institut Fédératif de Recherche 30, Hôpital Purpan, 31059 Toulouse, France; and <sup>§</sup>Department of Molecular, Cell, and Development Biology, Sinsheimer Laboratories, University of California, Santa Cruz, CA 95064

Submitted December 13, 2005; Revised April 13, 2006; Accepted April 18, 2006  
Monitoring Editor: Jean Gruenberg


Membrane dynamics is necessary for cell homeostasis and signal transduction and is in part regulated by phosphoinositides. Pikfyve/Fab1p is a phosphoinositide kinase that phosphorylates phosphatidylinositol 3-monophosphate into phosphatidylinositol-3,5-bisphosphate [PtdIns(3,5)P<sub>2</sub>] and is implicated in membrane homeostasis in yeast and in mammalian cells. These two phosphoinositides are substrates of myotubularin phosphatases found mutated in neuromuscular diseases. We studied the roles of phosphatidylinositol phosphate kinase 3 (PPK-3), the orthologue of PIKfyve/Fab1p, in a multicellular organism, *Caenorhabditis elegans*. Complete loss of *ppk-3* function induces developmental defects characterized by embryonic lethality, whereas partial loss of function leads to growth retardation. At the cellular level, *ppk-3* mutants display a striking enlargement of vacuoles positive for lysosome-associated membrane protein 1 in different tissues. In the intestine, RAB-7-positive late endosomes are also enlarged. Membranes of the enlarged lysosomes originate at least in part from smaller lysosomes, and functional and genetic analyses show that the terminal maturation of lysosomes is defective. Protein degradation is not affected in the hypomorphic *ppk-3* mutant and is thus uncoupled from membrane retrieval. We measured the level of PtdIns(3,5)P<sub>2</sub> and showed that its production is impaired in this mutant. This work strongly suggests that the main function of PPK-3 is to mediate membrane retrieval from matured lysosomes through regulation of PtdIns(3,5)P<sub>2</sub>.

## INTRODUCTION

In eukaryotic cells, spatiotemporal regulation of cellular organization and cell communication requires tightly regulated second messengers and microdomains. Phosphoinositides (PIs) are second messengers implicated in transduction pathways and membrane trafficking. Seven distinct PIs can be produced by phosphorylation of phosphatidylinositol at different positions. They recruit specific protein effectors leading to

their localization to their site of action (Wenk and De Camilli, 2004). Several lipid-binding protein domains have been described (Simonsen *et al.*, 2001). For example, phosphatidylinositol-3,4,5-triphosphate recruits Akt/protein kinase B through its pleckstrin homology domain at the plasma membrane, leading to phosphorylation of effectors and activation of downstream pathways, whereas phosphatidylinositol 3-monophosphate [PtdIns(3)P] binds to the FYVE domains of early endosomal antigen EEA1 and Hrs, proteins implicated respectively in early endosome fusion and in receptor sorting in multivesicular bodies (MVBs) (Gruenberg and Stenmark, 2004). PtdIns(3)P is found mainly on early endosomes and internal membranes of MVBs, whereas phosphatidylinositol-3,5-bisphosphate [PtdIns(3,5)P<sub>2</sub>] is on the external membrane of MVBs. These PIs regulate endocytosis and thus protein transport and degradation. For example, growth factors receptors are internalized after stimulation and their signals are down-regulated by their degradation in lysosomes (Miaczynska *et al.*, 2004). Receptors are first endocytosed into early endosomes where they are sorted: they are either recycled back to the plasma membrane or internalized into the lumen of maturing MVBs. Lysosomes could be formed either through maturation of late endosome/MVB by Rab conversion as in the case of the maturation from early to late endosomes (Rink *et al.*, 2005), through fusion into a hybrid organelle and fission (Treusch *et*

This article was published online ahead of print in *MBC in Press* (<http://www.molbiolcell.org/cgi/doi/10.1091/mbc.E05-12-1120>) on April 26, 2006.

 The online version of this article contains supplemental material at *MBC Online* (<http://www.molbiolcell.org>).

Address correspondence to: Jocelyn Laporte (mtm@igbmc.u-strasbg.fr).

Abbreviations used: CUP, coelomocyte uptake defective; LGG-1, LC3, GABARAP, and GATE-16; MVB, multivesicular body; PIKfyve, phosphatidylinositol kinase Fab1p, YoTb, Vac1p, EEA1, Fab1p: formation of aploid and binucleate cells; LMP, lysosome-associated membrane protein; PPK-3, phosphatidylinositol phosphate kinase 3; PtdIns(3)P, phosphatidylinositol-3-monophosphate; PtdIns(3,5)P<sub>2</sub>, phosphatidylinositol-3,5-bisphosphate; RME, receptor-mediated endocytosis.

al., 2004), or by kiss-and-run between late endosomes and existing lysosomes (Bright *et al.*, 2005). Numerous and highly regulated exchanges exist between different compartments. Transported proteins are concentrated on microdomains, and membrane exchange is initiated by budding and fission. In the case of the endosome-to-Golgi retrograde transport, membrane retrieval is regulated by the retromer complex (Griffin *et al.*, 2005; Seaman, 2005). This is controlled at least by the Vps34p, a phosphoinositide-3 kinase, indicating a role for PIs in retrograde transport (Burda *et al.*, 2002).

The phosphorylation status of PIs is regulated by lipid kinases and phosphatases. Mammalian PIKfyve, the phosphatidylinositol-3-phosphate 5-kinase type III (PIP5K3), transforms PtdIns(3)P into PtdIns(3,5)P<sub>2</sub> (Shisheva, 2001). These two PIs are substrates of myotubularin phosphatases, which are mutated in several neuromuscular disorders (Laporte *et al.*, 1996; Bolino *et al.*, 2000; Azzedine *et al.*, 2003; Laporte *et al.*, 2003; Senderek *et al.*, 2003). In addition, PIKfyve was recently found mutated in patients with a corneal dystrophy (Li *et al.*, 2005). PIKfyve was shown to be implicated in endomembrane integrity and in the control of fluid phase endocytosis (Ikonomov *et al.*, 2002, 2003a). Overexpression of a kinase-defective PIKfyve<sup>K1831E</sup> mutant in mammalian cells produced abnormal vesicles, which were described as enlarged MVBs. However, this did not affect epidermal growth factor receptor degradation. In 3T3-L1 adipocytes, PIKfyve enhanced insulin-stimulated GLUT4 vesicle translocation to the plasma membrane (Berwick *et al.*, 2004). The importance of this phosphoinositide pathway in membrane trafficking has also been highlighted in yeast by the study of Fab1p, the orthologue of PIKfyve (Efe *et al.*, 2005). Fab1p is important for vacuole size regulation, protein sorting at MVBs, and vacuole acidification (Gary *et al.*, 1998; Odorizzi *et al.*, 1998). The yeast vacuole, which is analogous to the mammalian lysosome, was enlarged in Fab1p mutants and defects in vacuolar inheritance have also been noted (Efe *et al.*, 2005). In wild-type yeast, PtdIns(3,5)P<sub>2</sub> increased upon hyperosmotic shock (Dove *et al.*, 1997), leading to vacuolar fragmentation (Bonangelino *et al.*, 2002), suggesting that Fab1p is also implicated in osmoregulation. Part of the roles of PIKfyve/Fab1p are transduced by PtdIns(3,5)P<sub>2</sub> effectors. These include Ent3p, Ent5p, and mVps24 for MVB sorting (Friant *et al.*, 2003; Whitley *et al.*, 2003) and Atg18p for membrane retrograde transport and partitioning of the vacuole (Dove *et al.*, 2004). Atg18p has also been implicated in membrane and protein retrieval from the preautophagosomal structures (Reggiori *et al.*, 2004). Discrepancies still exist between yeasts and mammalian cell systems concerning the roles of PIKfyve/Fab1p on receptor degradation and signal transduction.

The roles of PIKfyve have never been investigated in vivo in higher eukaryotes. We describe here our studies on phosphatidylinositol phosphate kinase 3 (PPK-3), the orthologue of PIKfyve/Fab1p in *Caenorhabditis elegans*, a multicellular organism with a complex endocytic machinery. *ppk-3* mutants have developmental defects and display a striking enlargement of lysosomes (a "swiss-cheese" like phenotype). These enlarged vacuoles are nonacidic, and protein degradation is not affected. Functional and genetic analyses showed that the defect lies in the maturation of formed lysosomes.

## MATERIALS AND METHODS

### *Caenorhabditis elegans* Strains and General Methods

*C. elegans* strains were derived from the wild-type Bristol strain N2. Worm cultures, genetic crosses, and other *C. elegans* methods were performed ac-

ording to standard protocols (Brenner, 1974). The following mutations and rearrangements were used: *ppk-3(mc46)*, *vac-2(n2668)*, *vac-2(n2835)* (this work), *cup-5(ar465)* (Fares and Greenwald, 2001), and *szT1* (provided by the *Caenorhabditis* Genetics Center, University of Minnesota, St. Paul, MN), which balances the right half of LG X and the left half of LGI. Transgenic strains used for this study are *cdIs36[punc-122::C31E10.7::GFP]* for endoplasmic reticulum, *cdEx88[pocl::gyMANS]* for Golgi, *pvl50[hmp-1::GFP]* for lysosomes, *cdEx49[punc-122::GFP::rab-5]* and *pvl572[pvha-6::GFP::rab-5]* (provided by B. Grant, Rutgers University, Piscataway, NJ; Chen *et al.*, 2006) for early endosomes, *bIs33[rme-8::GFP]* for late endosomes (provided by B. Grant; Zhang *et al.*, 2001), *cdIs67[punc-122::GFP::rab-7]* and *pvl5429[pvha-6::RFP::rab-7]* (provided by B. Grant; Chen *et al.*, 2006) for late endosomes and lysosomes, and *Ex[lgg-1::GFP]* for autophagosomes [provided by B. Levine (Columbia University College of Physicians and Surgeons, New York); Melendez *et al.*, 2003]. *cdEx46[punc-122::2XFYVE::GFP]* expresses a probe which specifically binds PtdIns(3)P. *bIs1[vit-2::GFP]* (provided by B. Grant), expressing a fusion between the yolk protein YP170 and green fluorescent protein (GFP), was used to monitor yolk degradation in embryos. Coelomocyte endocytosis was assayed using *arl337[pmyo-3::ssGFP]* and *cdIs5[pmyo-3::ssDsRed2]*.

*ppk-3* genomic DNA (8 kb), including 1.5 kb of the upstream intergenic region and the whole *ppk-3* gene, were PCR-amplified using the primers F1 (5'-CATGGATCCTACTGAAATTTGCCATATGGGG-3') and R1 (5'-ATTGGATCCTATAAGACCTAATTGATCCGAG-3') containing BamHI restriction sites and cloned in the *C. elegans pmyo3::YFP* vector pPD136-64 [provided by A. Fire (Stanford University School of Medicine, Stanford, CA)]. From this construct, we PCR amplified a fragment containing 1.5 kb of the intergenic region, the *ppk-3* genomic DNA fused with yellow fluorescent protein (YFP) in its C terminal part and the 3'-untranslated region of *unc-54* using the primers F1 and R2 (5'-AAGGGCCGTACGGCCGACTAGTAGG-3'). The resulting PCR-amplified *ppk-3::YFP* fusion (40 ng/μl) was coinjected with pRF4 (100 ng/μl) as a transformation marker into N2 and *ppk-3(n2668)* young animals to determine *ppk-3* expression and to test the rescue of the phenotype.

Lethality assays were done by allowing adult hermaphrodites to lay eggs for 4 h and scoring the number of eggs. For embryonic lethality, larvae were counted 15 h later, and postembryonic lethality was assayed 48 h after egg laying. Lethality percentages were calculated by dividing the number of deduced dead animals (for embryonic lethality, number of eggs laid – number of larvae at 15 h; for postembryonic lethality, number of larvae at 15 h – number of worms alive at 48 h) by the number of eggs laid for each indicated phenotype. The growth delay was assayed by determining the stages of live animals present on the Petri plates 3 and 5 d after egg laying.

RNA interference (RNAi) against *rab-7* was performed by the feeding method (Timmons and Fire, 1998) and the corresponding clone W03C9.3 is part of the RNAi library of J. Ahringer (University of Cambridge, Cambridge, United Kingdom).

### Isolation and Identification of *ppk-3* Mutants

The allele *ppk-3(mc46)* was isolated by PCR screening, after 25 mM ethane methyl sulfonate (EMS)-induced mutagenesis on wild-type L4 hermaphrodites (Wei *et al.*, 2002), by using two pairs of nested primers located around the active site of *ppk-3*: F1 (5'-TCACCACCGACACAATCTACC-3'), R1 (5'-CAGTATCAAAGCATCAATGATTTC-3'), F2 (5'-ACTAATCAGAATCAATGCTCCG-3'), and R2 (5'-TCACACAAGTGAATTGGTAGAC-3'). The mutations *vac-2(n2668)* and *vac-2(n2835)* were isolated in an EMS screen for larval lethal mutants with defects in morphogenesis and tissue integrity (Chisholm, unpublished results). *ok1150* was provided by the *Caenorhabditis* Genetics Center. The mutations affecting *ppk-3(mc46)*, *vac-2(n2668)*, and *vac-2(n2835)* alleles were identified by sequencing each *ppk-3* exon after PCR amplification. Animals segregating *mc46* or *n2668* or *n2835* were outcrossed eight times to wild-type animals, and *mc46* was balanced with *szT1*. Complementation tests between *mc46* and *n2668* were performed by crossing *n2668/0* males with *mc46/mc46* hermaphrodites. The *mc46* mutation was followed through genetic crosses by PCR using three primers: two around the deletion F (5'-ACA-GATGGATGATGGGGAAA-3') and R (5'-CGGAAAGTACGAGTCGATGG-3'), and one hybridizing into the deletion region F(5'-TGTATAAGTCAAGTCAAGTGAAC-3'). *n2668* is a missense mutation, which destroys a BanII restriction site. We then followed the mutation by cutting with BanII the fragment PCR-amplified using F (5'-ATGTCACGGTTTGAGATTTCAG-3') and R (5'-AGGAAGTGGCTGTCATTGC-3').

### Immunofluorescence

For anti-GFP immunostaining of embryos, mixed staged wild-type or mutant embryos were mounted on polylysine-coated slides, freeze cracked in liquid nitrogen, and fixed in successive baths in -20°C methanol, -20°C acetone, and graded acetone:phosphate-buffered saline mixes. Embryos were then incubated overnight with a monoclonal anti-GFP antibody (Institut de Génétique et de Biologie Moléculaire et Cellulaire, Euromedex, Souffelweyersheim, France) diluted 1/1000 in phosphate-buffered saline (PBS)/0.5% Tween/0.1% bovine serum albumin (BSA), washed with PBS/0.5% Tween/0.1% BSA, incubated overnight with a Cy3-coupled secondary antibody, washed with PBS/0.5% Tween containing 1 μg/ml final 4,6-diamidino-2-phenylindole (DAPI) to locate all nuclei, and viewed with a confocal microscope.

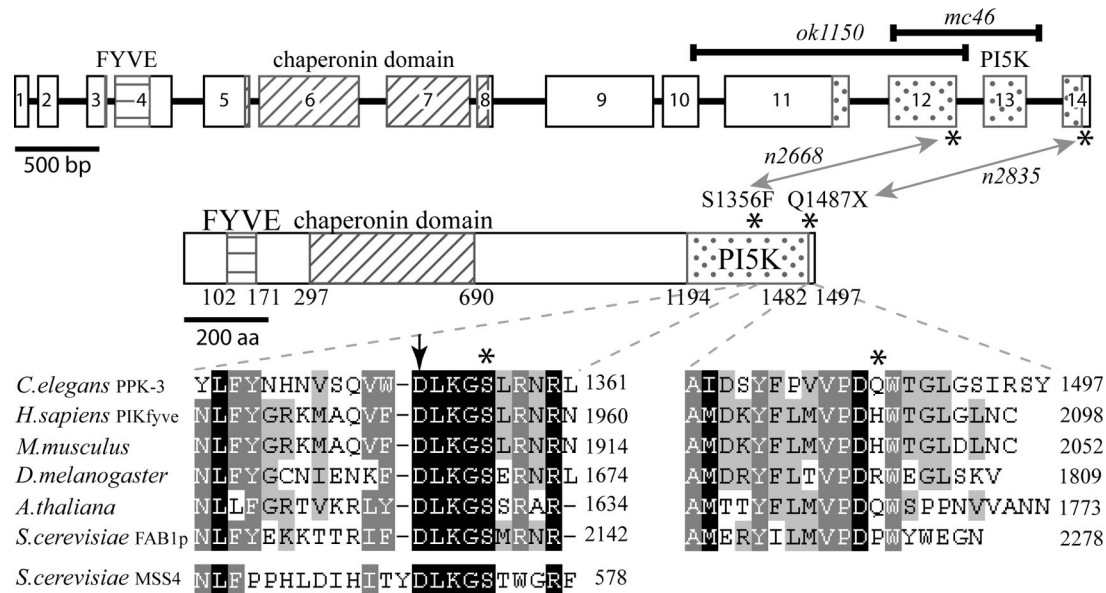


**Figure 1.** *ppk-3* gene, protein, and mutations. From sequence conservation analysis, we predicted a new sequence for the *ppk-3* gene and protein. At the top is depicted the genomic structure of the gene encompassing 14 exons (boxed) and encoding a 1497-amino acid protein. Predicted intron 6 from VF11C1L.1 (<http://www.wormbase.org/>) is found in cDNA clones, and the N-terminal was extended based on protein conservation. Protein domains and their encoding sequences, predicted by the SMART database (<http://smart.embl-heidelberg.de/>; Schultz *et al.*, 2000) are indicated with boxes: horizontal lines for the FYVE domain (Fab1p, YoTb, Vac1p, EEA1), diagonal lines for the TCP-1/cpn60 chaperonin family domain and dots for the lipid kinase domain. Deletions are indicated with bars above the genomic structure, and missense and stop mutations are reported with stars on the protein. Corresponding alleles are indicated in italic. Below, we aligned, with ClustalX (Thompson *et al.*, 1997), the two regions containing point mutations with orthologues of PPK-3; on the left, the region contains the catalytic loop and magnesium coordination residues (DLKGS, underlined), and the region on the right corresponds to the terminal end of some PIKfyve/Fab1p protein family members, except for *Arabidopsis thaliana* whose full size is 1791 amino acids. Proteins sequences used are worm VF11C1L.1 (see Supplemental Material), human PIKfyve (NP\_055855), mouse PIKfyve (NP\_035216), *Drosophila* CG6355 (NP\_611269), thale cress At3g14270 (NP\_188044), and yeast Fab1p (NP\_116674). We added the region containing the catalytic loop of Mss4 (NP\_010494), the only yeast orthologue of PI4P5K class I and II. The arrow indicates the position of the missense of the *S. cerevisiae* Fab1p kinase-dead mutant.

Anti-GFP immunostaining of adult worms was done according to the protocol of McIntire with minor modifications (McIntire *et al.*, 1992). Briefly, wild-type and mutant young adults were fixed 1 d in 4% paraformaldehyde and then incubated overnight in 5%  $\beta$ -mercaptoethanol, 0.125 M Tris, pH 6.9, and 1% Triton at 37°C. The cuticle was disrupted by treatment with 1000 U/ml collagenase type IV (Sigma-Aldrich, St. Louis, MO) in 100 mM Tris, pH 7.5, 1 mM CaCl<sub>2</sub>, for 30 min at 37°C, and membranes were permeabilized by an incubation of 1 h in 0.125 M Tris, pH 6.9, 1% Triton. Worms were then incubated 24 h with a monoclonal anti-GFP antibody (Institut de Génétique et Biologie Moléculaire et Cellulaire, Euromedex) diluted 1/1000, washed, incubated 4 h with a Cy3-coupled secondary antibody, washed, and viewed with a confocal microscope. Antibodies were diluted in PBS/0.5% Triton/0.5% BSA, and washes were done with PBS/0.5% Triton/0.3% BSA.

For anti-PtdIns(3,5)P<sub>2</sub> immunostaining, mixed staged embryos of wild-type and mutants were mounted and freeze cracked, incubated in -20°C methanol, fixed overnight in 1% paraformaldehyde, and then incubated overnight with a monoclonal anti-PtdIns(3,5)P<sub>2</sub> antibody (Echelon Biosciences, Salt Lake City, UT) diluted 1/40 (12.5  $\mu$ g/ml final) in PBS/0.1% BSA without any detergent. Embryos were then washed, incubated overnight with a fluorescein isothiocyanate-coupled goat anti-mouse secondary antibody (Beckman Coulter France, Roissy CDG cedex, France), washed with PBS/DAPI, and viewed with a confocal microscope. Experiments were done twice.

### Confocal Microscopy

Animals were mounted on 2% agarose pads with 0.2% tricaine/0.02% tetraanisole in M9. For differential interference contrast, we used a Zeiss Axioplan microscope coupled to a CoolsNAP camera (Photometrics, Tucson, AZ) under a PlanApo 10 $\times$  objective. For confocal imaging, we used a Leica SP2-AOBS confocal microscope with an argon 488 excitation to visualize the green dyes and the autofluorescence of worm intestine and a HeNe 543 excitation for the red dyes. Pictures of the same experiment were taken at the same exposure. We then processed images with the Tcstk software (Jean-Luc Vonesch, Institut de Génétique et de Biologie Moléculaire et Cellulaire) and edited pictures using the Dvrtk software (Jean-Luc Vonesch, Institut de Génétique et de Biologie Moléculaire et Cellulaire) and Adobe Photoshop 7.0. Fluorescence

intensities were quantified in whole embryos using the Leica Confocal software (Leica, Wetzlar, Germany). Dot-like structures of the anti-PtdIns(3,5)P<sub>2</sub> staining in embryos were scored using the MetaMorph software (Molecular Devices, Sunnyvale, CA) in squares of 280  $\mu$ m<sup>2</sup>. The average value obtained with 25 different embryos per strain was calculated and difference between wild-type and *ppk-3(n2668)* mutant was tested with a Student's *t* test.

### Electron Microscopy

Worms were processed for electron microscopy as described previously (Michaux *et al.*, 2000). Briefly, young adults were sectioned and fixed for 24 h in 2.5% glutaraldehyde in 0.1 M sodium cacodylate buffer, pH 7.2, at 4°C. Worms were postfixed for 5 h with 2% osmium tetroxide in the same sodium cacodylate buffer at 4°C. Animals were dehydrated in graded alcohol:water mixes and then embedded in Epon. Ultrathin sections of 70 nm were contrasted with uranyl acetate and lead citrate. Sections were observed with a Philips CM12 electron microscope. At least eight animals per strain were examined.

### Endocytosis Assays and Time Course

As described previously (Treichl *et al.*, 2004), Texas-Red BSA (TR-BSA; Sigma) was injected at 1 mg/ml in water into the body cavity of wild-type or *n2668* young adult hermaphrodites expressing LMP-1::GFP. At defined time points, animals were mounted on slides, put on ice to stop endocytosis, and fluid-phase internalization of the dye into the coelomocytes was viewed with a confocal microscope. For each time point, similar results were obtained with the coelomocytes of at least six different worms. LysoTracker Red DND-99 (Invitrogen, Carlsbad, CA) is a red fluorescent dye that selectively accumulates in cellular compartments with low internal pH. LysoTracker Red DND-99 was injected into the pseudocoelomic space of wild-type and mutant worms expressing LMP-1::GFP at 0.4 mM in M9 buffer, and its localization inside the coelomocytes was viewed 4 h after injection with a confocal microscope at a 514-nm excitation wavelength and a 580- to 660-nm range emission. The dynamic of the abnormal vacuole biogenesis in *ppk-3(mc46)* and *ppk-3(n2668)* mutant coelomocytes was followed through 20 min. Focal plane

was changed during experiment to ensure proper visualization of the biggest diameter of the fusing vacuole observed, and pictures were taken at key time points.

### Lipid Extraction and Analysis

Worms were collected and washed in phosphate-free RPMI-1640 medium at 20°C and labeled with 1 mCi/ml [<sup>32</sup>P]orthophosphate (GE Healthcare, Little Chalfont, Buckinghamshire, United Kingdom) during 12 h in phosphate-free RPMI-1640 medium at 20°C. <sup>32</sup>P-labeled worms were then washed once in phosphate-free RPMI-1640 medium at 20°C, and lipids were immediately extracted following the modified procedure of Bligh and Dyer (1959). Lipids were then separated by TLC (Merck, Nogent-sur-Marne, France) using CHCl<sub>3</sub>/CH<sub>3</sub>COCH<sub>3</sub>/CH<sub>3</sub>COOH/H<sub>2</sub>O [80/30/26/24/14 (vol/vol)] as a solvent. The spots corresponding to [<sup>32</sup>P]PtdInsP<sub>2</sub> were visualized by a PhosphorImager 445 SI (GE Healthcare) using appropriate standards, scraped off, deacylated, and analyzed by high-performance liquid chromatography (HPLC) on a Whatman Partisphere 5 SAX column (Whatman International, Maidstone, United Kingdom) as described previously (Payrastré, 2004).

## RESULTS

### Developmental and Vacuolar Defects in *ppk-3* Mutants

To identify the *Caenorhabditis elegans* orthologue of PIKfyve/Fab1p, we compared the human and *Saccharomyces cerevisiae* protein sequences to the *C. elegans* predicted transcript and genomic sequences using tblastn. We identified VF11C1L.1 (also named *ppk-3*) on the X chromosome as the *C. elegans* orthologue. We updated the predicted sequence found in the database by sequencing cDNA clones [OSTR10224F1, provided by M. Vidal (Dana-Farber Cancer Institute, Boston, MA)], by comparison of expressed sequence tags on WormBase [yk246g4.5, yk1185g10.5 from Y. Kohara (National Institute of Genetics, Shizuoka, Japan)] to confirm that the predicted intron 6 is indeed coding, and by comparison of the PIKfyve protein family sequences through evolution to extend the N-terminal sequence. We predicted that the *ppk-3* gene encompasses 14 exons and encodes a 1497-amino acid-long protein with a start ATG codon at position 12 975 563 on the X chromosome (Figure 1 and Supplemental Figure 1). Like its orthologues in yeast, plants, and other eukaryotes, PPK-3 has an N-terminal Fab1p, YOTB, Vac1p, EEA1 (FYVE) domain, which might bind to PtdIns(3)P, a domain related to the Cpn60/TCP-1 chaperonin family, and a lipid kinase domain related to yeast Mss4 and class I and II phosphatidylinositol kinases. The protein is, however, significantly smaller than the human protein and lacks the Dishevelled, Egl-10, and Pleckstrin domain found between the FYVE and the chaperonin-like domains in *Drosophila*, mouse and human orthologues.

To investigate the expression pattern of *ppk-3*, we fused genomic sequence, from 1.5 kb upstream of the initiation codon to the last codon, with YFP and observed, at all stages, a mosaic expression in the pharynx and in the nervous system: some head and tail neurons, some neurons of the dorsal and ventral nerve cords, and some commissures. At early larval stages, an intestinal expression was detected (Supplemental Figure 2). This is compatible with an expression pattern determined using a *ppk-3::GFP* transcriptional fusion *sEx13072* (McKay *et al.*, 2003). In neurons, our *ppk-3::YFP* fusion protein was localized as cytoplasmic dots in cell bodies and axons. In the intestine, PPK-3 displayed a diffuse localization with some punctate staining (Supplemental Figure 2).

We screened by PCR for *ppk-3* mutants generated by EMS mutagenesis and isolated a deletion mutant (*mc46*) lacking most of the kinase domain ( $\Delta$ 5213-6077 on the genomic sequence) (Figure 1). This mutant displayed large vacuoles and by comparison with this swiss-cheese phenotype, we identified two other mutants, *n2668* and *n2835*, mapping to the same chromosomal region as the *ppk-3* gene, which were

Strain	Emb Let	Post-Emb Let	Growth delay
<i>mc46/mc46</i> (n=2059)	99,9%	0,1%	-
<i>n2668/n2668</i> (n=533)	27%	8%	15% of alive animals are not adult at 5 days.
<i>n2835/n2835</i> (n=306)	5%	1%	No
<i>mc46/n2668</i> (n=168)	39%	6%	56% of alive animals are L1 at 3 days.
<i>mc46/+</i> or <i>mc46/0</i> (from $\phi$ <i>mc46/mc46</i> $\times$ <i>+/+</i> ) (n=512)	54% (~males)	0%	No
<i>n2668/n2668</i> Ex[ <i>ppk-3</i> ] (n=513)	2%	0%	No

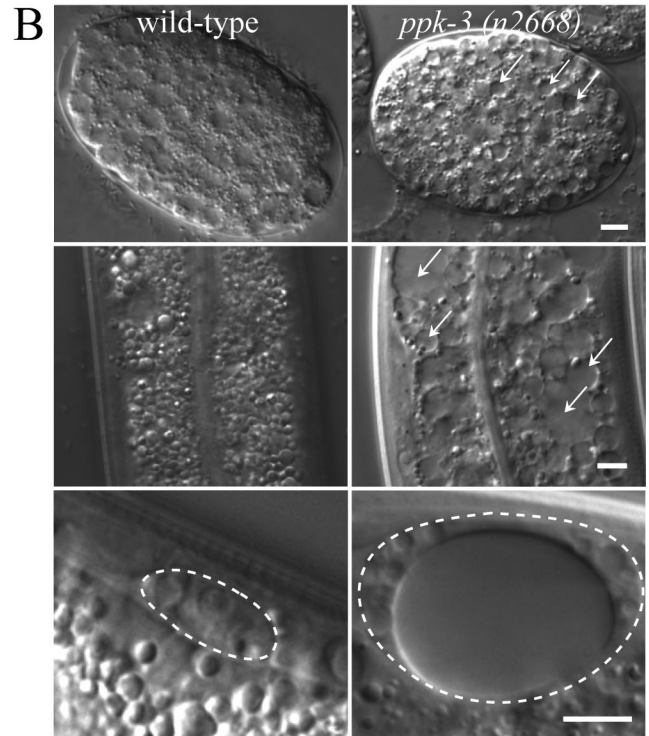


**Figure 2.** Developmental defect and swiss-cheese phenotype. (A) Lethality and growth delay of different *ppk-3* mutants. n, number of eggs laid; Emb Let, embryonic lethality; Post-Emb Let, postembryonic lethality. Values reflect the lethality compared with n. The embryonic lethality (54%) in the progeny of *mc46/mc46* hermaphrodites crossed with wild-type +/0 males probably corresponds to the *mc46/0* males. (B) Nomarski pictures of wild-type and *ppk-3* (*n2668*) mutants: eggs (top), L4 larva intestine (middle), and coelomocytes (bottom, circled). Arrows indicate some vacuoles. Bar, 5  $\mu$ m.

obtained by EMS mutagenesis and screened for larval lethal mutants with defects in morphogenesis and tissue integrity. *n2668* displayed enlarged vacuoles similar to *mc46* as monitored by Nomarski optics (Figure 2B). *ok1150* ( $\Delta$ 4027-5640 on the genomic sequence) was created by the *C. elegans* Gene Knockout Consortium. There was no allelic complementation between *mc46* and *n2668* (Figure 2A) nor between *n2668* and *n2835*. *n2668* causes a serine-to-phenylalanine (S1356F) change within the conserved catalytic loop DLKGS of the kinase domain, close to the aspartate mutated in the *S. cerevisiae* kinase dead Fab1p mutant (D2134R; Gary *et al.*, 1998). *n2835* causes a nonsense mutation (Q1487X), which removes the last 11 amino acids conserved in mammals (Figure 1).

These different mutants can be arranged in an allelic series composed of strong mutants (*mc46* and *ok1150*), a hypomorphic mutant (*n2668*), and a weak hypomorphic mutant (*n2835*) (Figure 2A). Homozygous *mc46* and *ok1150* animals laid by heterozygous mothers were viable but displayed

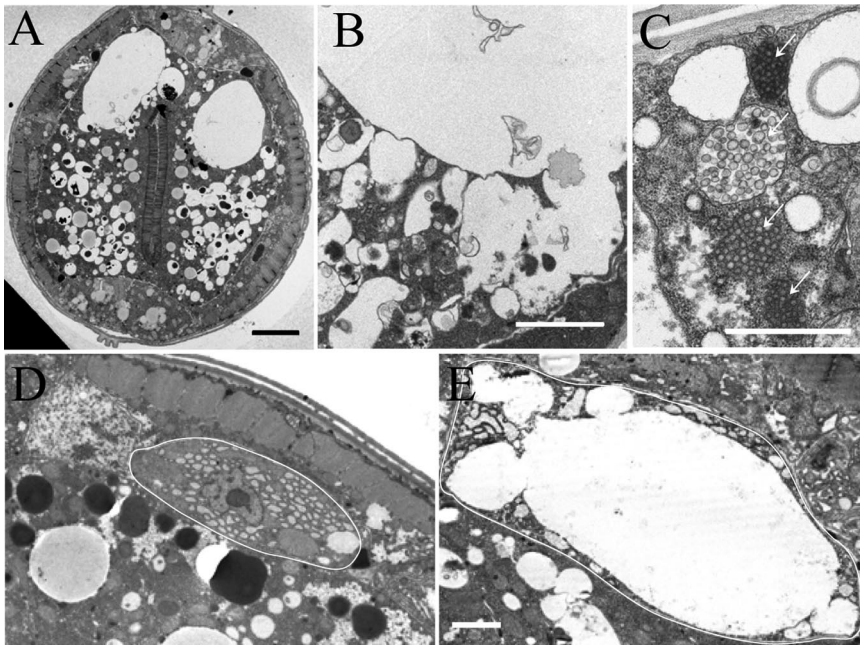


**Figure 3.** Abnormal vacuoles and membrane defects in *ppk-3(n2668)* mutant. Electron microscopy of wild-type and *ppk-3(n2668)* mutant young adults. (A) General view of a section from a *ppk-3(n2668)* mutant. Intestinal vacuoles are of different sizes and contain either membranes or condensed material. Bar, 5  $\mu$ m. (B) Zoom on intestinal vacuoles of a *ppk-3(n2668)* mutant. Vacuoles are surrounded by a membrane and show perturbed figures. Bar, 2  $\mu$ m. (C) Multivesicular bodies in the epidermis of a *ppk-3(n2668)* mutant. They are of normal size and are indicated with arrows. Bar, 1  $\mu$ m. (D and E) Coelomocytes of a wild-type (D) and a *ppk-3(n2668)* mutant (E) animal, surrounded by a white line. Note that the endoplasmic reticulum is elaborate, both in wild-type and mutant coelomocytes. Bar, 2  $\mu$ m.

numerous vacuoles, which filled a large part of the body. These homozygous progeny laid eggs that also contained vacuoles, did not hatch, and died at different embryonic stages. This maternal effect was not strict because it was rescued in heterozygous progeny obtained by crossing the viable homozygous mutants *mc46/mc46* with wild-type +/0 males: the 46% worms that lived were all *mc46/+* hermaphrodites, and the 54% dead eggs corresponded probably to the *mc46/0* males (Figure 2A). *n2668* also displayed a developmental defect: 27% embryonic lethality, 8% postembryonic lethality. Viable *n2668* animals had growth retardation as they reached adult stage up to 2 d later than the wild-type (wild-type animals are adults 2 d after hatching) (Figure 2A). Compared with *n2668*, *n2835* presented a reduced lethality and no growth retardation (Figure 2A). Both mutants displayed abnormal vacuoles of different sizes, which occurred at the one-cell stage in *n2668*. In *n2668* larvae and adult mutants, vacuoles were present in intestine, epidermis, coelomocytes (one big vacuole), and to a lesser extent in the pharynx (Figure 2B). To confirm that the observed phenotypes are due to mutations in *ppk-3*, we injected the *ppk-3::GFP* fusion construct into *n2668* mutants and obtained a rescue of the developmental defects (Figure 2A) and vacuolar phenotypes (our unpublished data). In conclusion, mutations of *ppk-3* in a multicellular eukaryote are responsible for developmental defects and for the appearance of abnormal vacuoles.

#### Abnormal Vacuoles in *ppk-3* Mutants Are Enlarged Lysosomes

To characterize these abnormal vacuoles and their origin, we used electron and fluorescent microscopy. The vacuoles were of different sizes and could reach up to 30% of the worm width (Figure 3A). This striking vacuolar phenotype did not prevent 65% of the worms from reaching adulthood in the *n2668* mutant. The vacuoles were surrounded by a membrane and were either empty, filled with membrane whirls in huge vacuoles, or electron-dense deposits in smaller vacuoles. We noted numerous pictures of aggregation and fusion between the vacuoles (Figure 3B). Normal

multivesicular bodies were visible in the epidermis of the *ppk-3* mutant (Figure 3C). Most of the coelomocytes were filled with a unique huge vacuole that leads to an increase of the cell size of approximately two- to fourfold (Figure 3E). These results suggested a defect of membrane trafficking in *ppk-3* mutants.

To better define the origin of the enlarged vacuoles, we focused our analysis on coelomocytes, which are scavenger cells harboring strong endocytic and degradation processes (Fares and Grant, 2002). We chose the *n2668* mutant, which is viable and has a missense alteration in the catalytic loop of the kinase domain, to focus on the impact of PI dysregulation. We crossed *n2668* with transgenic worms expressing specific markers of different endocytosis and membrane compartments. There was no difference in Golgi (mannosidase II) and endoplasmic reticulum (C31E10.7 cytochrome *b*<sub>5</sub>) patterns between wild-type and mutant (our unpublished data). The endocytic markers, RAB-5 for early endosomes, and RME-8 for late endosomes (Zhang *et al.*, 2001), did not label the enlarged vacuole (Figure 4). In contrast, LMP-1, a lysosomal marker orthologous to human lysosomal-associated membrane protein 1 (Kostich *et al.*, 2000), always stained the membrane of the enlarged vacuoles, strongly suggesting a lysosomal identity. We obtained similar results for LMP-1 in the *mc46* mutant. RAB-7 weakly labeled the enlarged vacuoles of the mutant (Supplemental Figure 3A). In *C. elegans*, RAB-7 labels not only late endosomes but also lysosomes because all the vacuoles accumulating the fluid-phase marker Texas-Red–coupled BSA after 24 h were positive for RAB-7 and LMP-1, whereas they were negative for RME-8 (Supplemental Figure 3B).

In the intestine of *n2668*, LMP-1 stained the bigger vacuoles, whereas the small abnormal vacuoles were negative for RAB-5 and positive for RAB-7 (Figure 5). In contrast to coelomocytes, there was also a slight enlargement of late endosomes in the intestine. LGG-1, an autophagosome marker orthologous to LC3 (Melendez *et al.*, 2003), showed aggregations distinct from the abnormal vacuoles in the intestine of the *ppk-3* mutant (Figure 4). Thus, *ppk-3* mutants

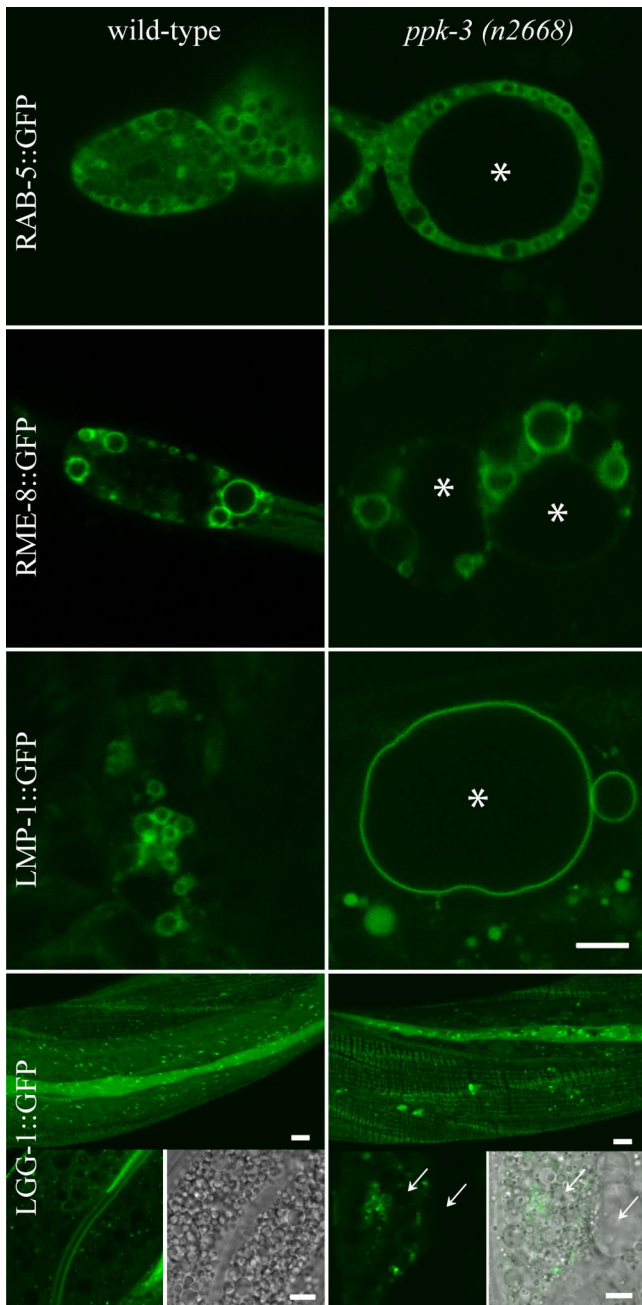


**Figure 4.** Morphological characterization of enlarged vacuoles in coelomocytes of *ppk-3(n2668)* worms. Confocal pictures of wild-type and *ppk-3(n2668)* coelomocytes expressing GFP-fused markers of early endosomes (RAB-5), late endosomes (RME-8), lysosomes (LMP-1), and autophagosomes (LGG-1). Enlarged vacuoles of *ppk-3* mutants are indicated by stars. All depicted images represent a single focal plane, except for LGG-1::GFP where a projection from confocal sections of the worm body is shown on the top. LGG-1 aggregates in the mutant do not colocalize with vacuoles (some indicated with arrows) visible on the corresponding Nomarski pictures. Bar, 5  $\mu$ m.

have enlarged lysosomes and a possible accumulation of autophagosomes.

To decipher the mechanism of enlargement of the lysosomes, we followed LMP-1-positive vacuoles in *ppk-3* mutants (*mc46* and *n2668*) over time in coelomocytes. We observed fusion between LMP-1-positive vacuoles. Smaller

vacuoles fused with the huge vacuole by two apparent mechanisms: either they fused rapidly or progressively (Figure 6A). For the first case, this led to an intermediate where the membrane of the huge vacuole was distorted after the fusion of the two membranes (fusion event within seconds). For the second case, the fusing vacuole decreased in size progressively (fusion event over a 20-min interval). Together, our results suggest that lack of *ppk-3* activity leads to enlargement of lysosomes, and addition of membranes is mediated through fusion with lysosomes.

#### *Involvement of ppk-3 in Terminal Maturation of Lysosomes*

To place more precisely the defect leading to lysosome enlargement, we first performed fluid uptake assays by injecting Texas-Red-coupled BSA into the body cavity of wild-type and *ppk-3* mutants. This fluorescent marker enters coelomocytes by fluid-phase-mediated endocytosis and is transported through the different endocytic compartments to the lysosomes. In wild-type animals, Texas-Red BSA was present in early endocytic compartments after 15 min, and we noted that it was concentrated in subdomains that are presumably budding domains (Treusch *et al.*, 2004). By 30 min, Texas-Red BSA was mostly in LMP-1-negative vesicles, which are late endosomes as verified with a time course using RME-8::GFP. From 30 min, it started to accumulate in lysosomes labeled with LMP-1::GFP (Figure 6B; our unpublished data). By 1 h and after 24 h of internalization, Texas-Red BSA had accumulated into most of the lysosomes (Figure 6B) and was absent from the RME-8::GFP late endosomes (Supplemental Figure 3B). In *ppk-3* mutants, the fluid phase endocytosis followed the same kinetics. Texas-Red BSA first localized to LMP-1-negative endosomes with concentrations in subdomains. By 30 min and 1 h, the Texas-Red BSA accumulated in normal LMP-1-positive compartments and in the LMP-1 large vacuoles. This is consistent with our finding that the large vacuoles are competent to fuse with other compartments. The fluorescent marker localization to the enlarged vacuole increased during the time course, indicating the progressive accumulation of the tracer (Figure 6B). Thus, lack of *ppk-3* activity does not prevent the fluid phase endocytosis to lysosomes, suggesting that the biogenesis of lysosomes is normal.

We further tested the maturation status of the enlarged lysosomes. We used worm strains expressing GFP or DsRed2 in the body wall muscle under the *myo-3* muscle-specific promoter. These fluorescent proteins are secreted into the body cavity and nonspecifically endocytosed primarily by coelomocytes. It is known that GFP is degraded, or bleached by the low pH, in mature lysosomes, whereas DsRed2 is stable (Fares and Grant, 2002; Patton *et al.*, 2005). The enlarged lysosomes of the *ppk-3(n2668)* mutant were strongly positive for DsRed2, whereas there was no accumulation of the GFP signal (Figure 7A). As a control, we used coelomocyte uptake defective (*cup-5*) mutants, which have a defect in lysosome formation (Treusch *et al.*, 2004). *cup-5* encodes a calcium-permeable channel orthologous to h-mucolipin-1, mutated in human mucopolipidosis type IV (Bargal *et al.*, 2000). In contrast to *ppk-3* mutants, *cup-5* mutants accumulated the GFP in aberrant late endosome/lysosome hybrid organelles. To confirm that *ppk-3* lies downstream of *cup-5*, we generated a double mutant *cup-5(ar465); ppk-3(n2668)*. GFP accumulated similarly in this double mutant compared with the single *cup-5* mutant (Figure 7A). CUP-5::GFP accumulated around the enlarged vacuoles of the *ppk-3*

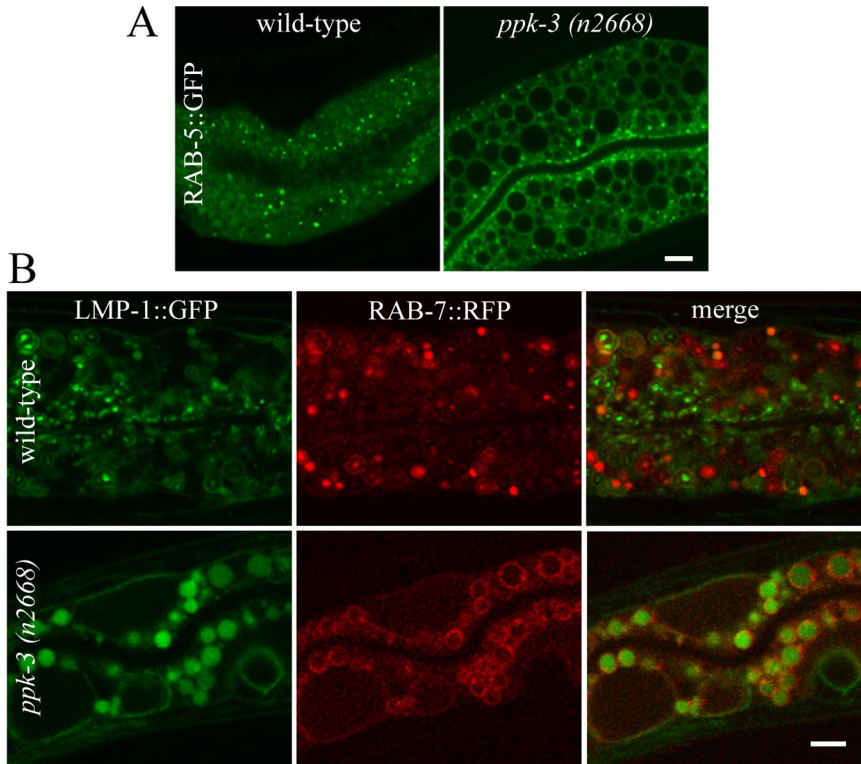


**Figure 5.** Morphological characterization of abnormal vacuoles in the intestine of *ppk-3*(n2668) worms. (A) Confocal pictures of wild-type and *ppk-3*(n2668) intestines expressing GFP-fused RAB-5, a marker of early endosomes. Bar, 5  $\mu$ m. (B) Confocal pictures of wild-type and *ppk-3*(n2668) intestines expressing LMP-1::GFP (green), a marker of lysosomes, and RAB-7::RFP (red), a marker of late endosomes and lysosomes. The merge picture of both panels is shown on the right. Vacuoles displaying internal green fluorescence in the intestine of *ppk-3*(n2668) mutant are enlarged autofluorescent granules. Bar, 5  $\mu$ m.

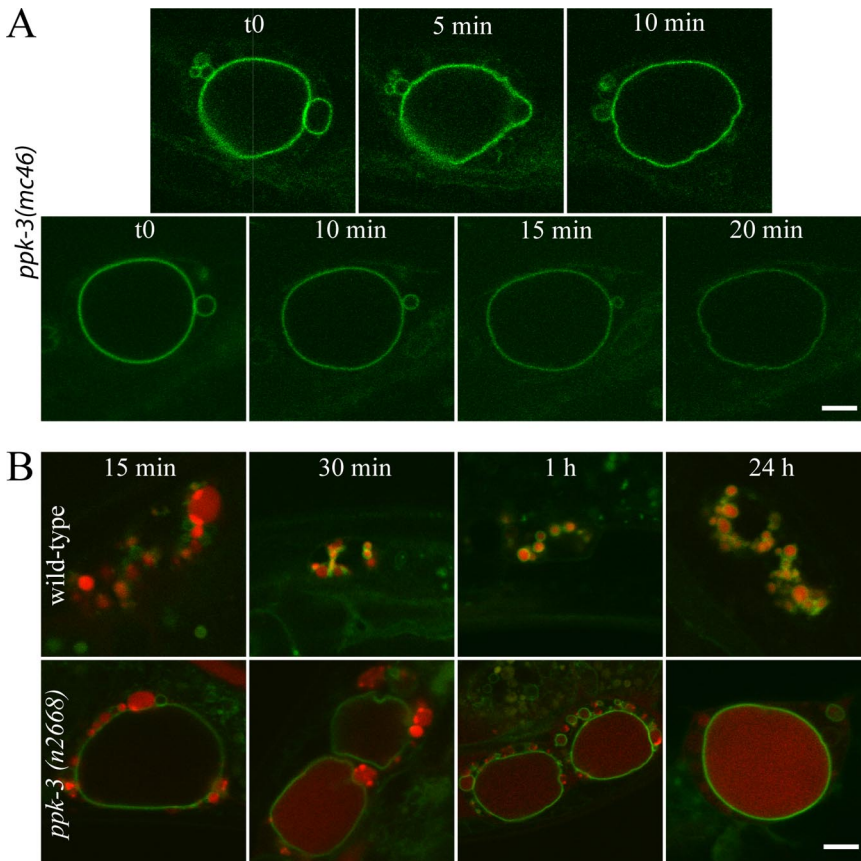


**Figure 6.** Biogenesis of the enlarged lysosomes and fluid uptake assays. (A) Time-lapse dynamic of LMP-1-positive vesicles in *ppk-3*(mc46) mutants. On the top, a lysosome fuses directly with the enlarged vacuole; the fusion happened within a second. At the bottom, fusion between both compartments occurs progressively over a 20-min interval. Focal plane was changed during experiment to insure that the fusing vacuole did not move out of the focal plane. (B) Time-course internalization of injected Texas-Red BSA through fluid uptake endocytosis in LMP-1::GFP-expressing coelomocytes. Bar, 5  $\mu$ m.

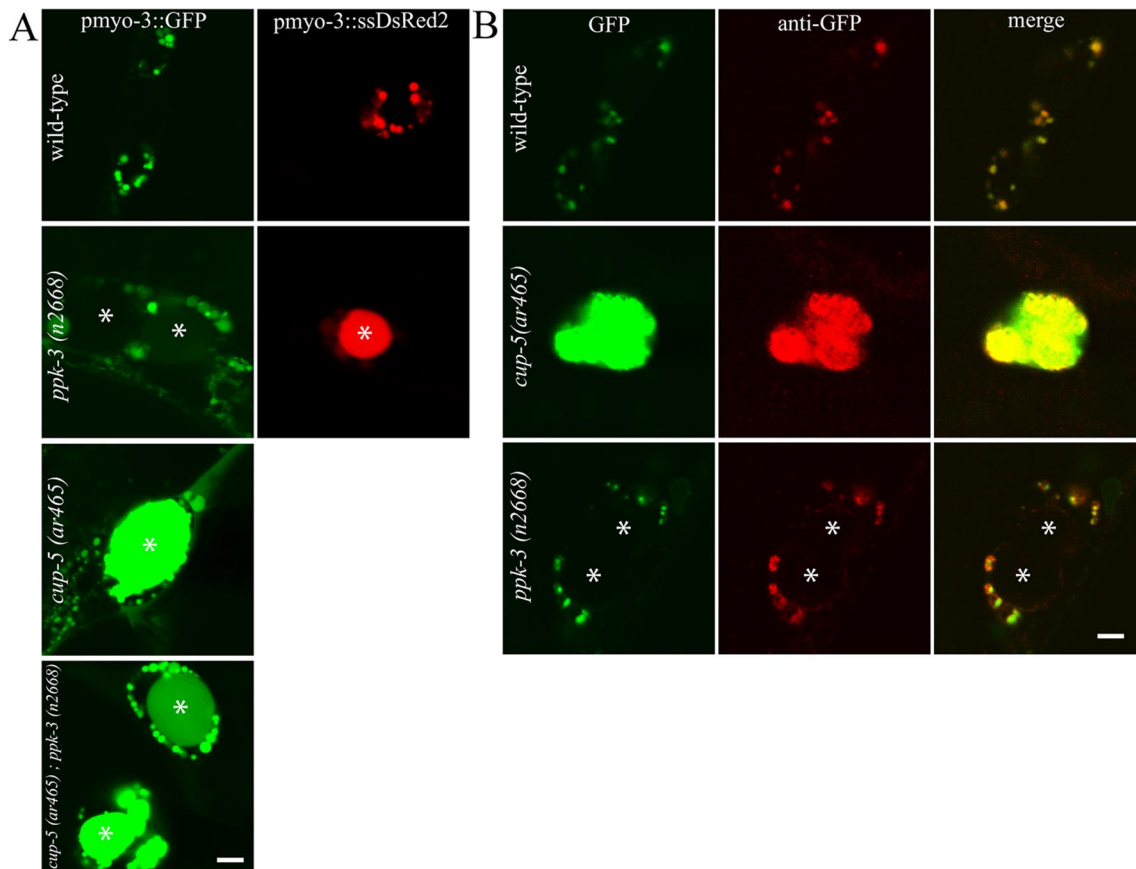


**Figure 7.** Differential GFP and ssDsRed2 accumulation in coelomocytes. (A) Confocal pictures of transgenic worms expressing GFP or ssDsRed2 under the *pmyo-3* muscle-specific promoter. Fluorescent proteins are secreted into the body cavity and internalized through endocytosis by coelomocytes. Differential accumulation of GFP and ssDsRed2 fluorescent proteins is recorded in wild-type, *ppk-3(n2668)*, *cup-5(ar465)* (gene implicated in lysosome biogenesis), and *cup-5;ppk-3* double mutant. Stars indicate the enlarged vacuoles of the different mutants. Bar, 5  $\mu$ m. (B) Confocal picture of wild-type, *cup-5(ar465)*, and *ppk-3(n2668)* mutants expressing GFP under the *pmyo3* muscle-specific promoter. The middle panel shows the corresponding anti-GFP labeling (red, Cy3) to rule out possible bleaching of the GFP. The merge picture is shown on the right panel. Enlarged vacuoles of the *ppk-3(n2668)* mutant are indicated by stars. Bar, 5  $\mu$ m.

mutants, and lethality increased in the double *cup-5(ar465); ppk-3(n2668)* (supplementary Figure 4), suggesting that these two proteins are implicated in the same process, PPK-3 being downstream of CUP-5. In conclusion, enlarged vacuoles of the *ppk-3* mutants are maturing lysosomes. It suggests that PPK-3 is not essential for lysosome formation but plays a role in lysosome maturation.

We further checked whether the enlarged lysosomes of the *ppk-3* mutants were functional by investigating protein degradation in the *ppk-3* mutant. Because the mutant worms expressing *pmyo-3::GFP* from Figure 7A did not accumulate the GFP in the enlarged lysosomes, we checked that the GFP was indeed degraded and not bleached. Anti-GFP immunostaining of the *ppk-3* mutant confirmed that GFP was degraded showing that, although there is no protein degradation in the enlarged hybrid organelles of *cup-5* mutants, protein degradation occurred in the enlarged lysosomes of the *ppk-3* mutants (Figure 7B).

As a second test for protein degradation, we monitored the presence and level of the yolk protein vitellin-2 (YP170) in embryos (Britton and Murray, 2004). Yolk proteins are synthesized by intestinal cells and transported to the oocytes to be used as amino acid source by the developing eggs. It was previously reported that cathepsin-L1 mutants and

worms fed with RNAi against *rab-7*, two genes implicated in lysosome formation and function, are defective for yolk protein processing and degradation, leading to an accumulation of YP170::GFP in abnormal vacuoles (Grant and Hirsh, 1999; Britton and Murray, 2004), as shown for *rab-7* RNAi in Figure 8A. We compared the fluorescence intensity of YP170::GFP in wild-type and *ppk-3* mutant transgenic embryos. No detectable difference was noted ( $p = 0.07$ ) (Figure 8, B and C). To rule out possible bleaching of the GFP fluorescence due to an acidic environment, we performed an anti-GFP immunostaining and obtained similar results ( $p = 0.29$ ) (Figure 8, B and C). This was sustained by the presence of autofluorescent granules in the intestine of *ppk-3* mutants, believed to correspond to lysosomes containing lipofuscin, a degradation product (Clokey and Jacobson, 1986).

Acidification was monitored by injection of LysoTracker Red DND-99 into the coelom of LMP-1::GFP-expressing worms. LysoTracker Red DND-99 fluoresces in acidic compartments and is retained in their membranes. In wild-type worms, all lysosomes were positive for LysoTracker Red DND-99, whereas in *ppk-3(n2668)* mutant, the enlarged vacuoles did not stain, suggesting that they were not acid (Figure 8D). Together, our results suggest that degradation



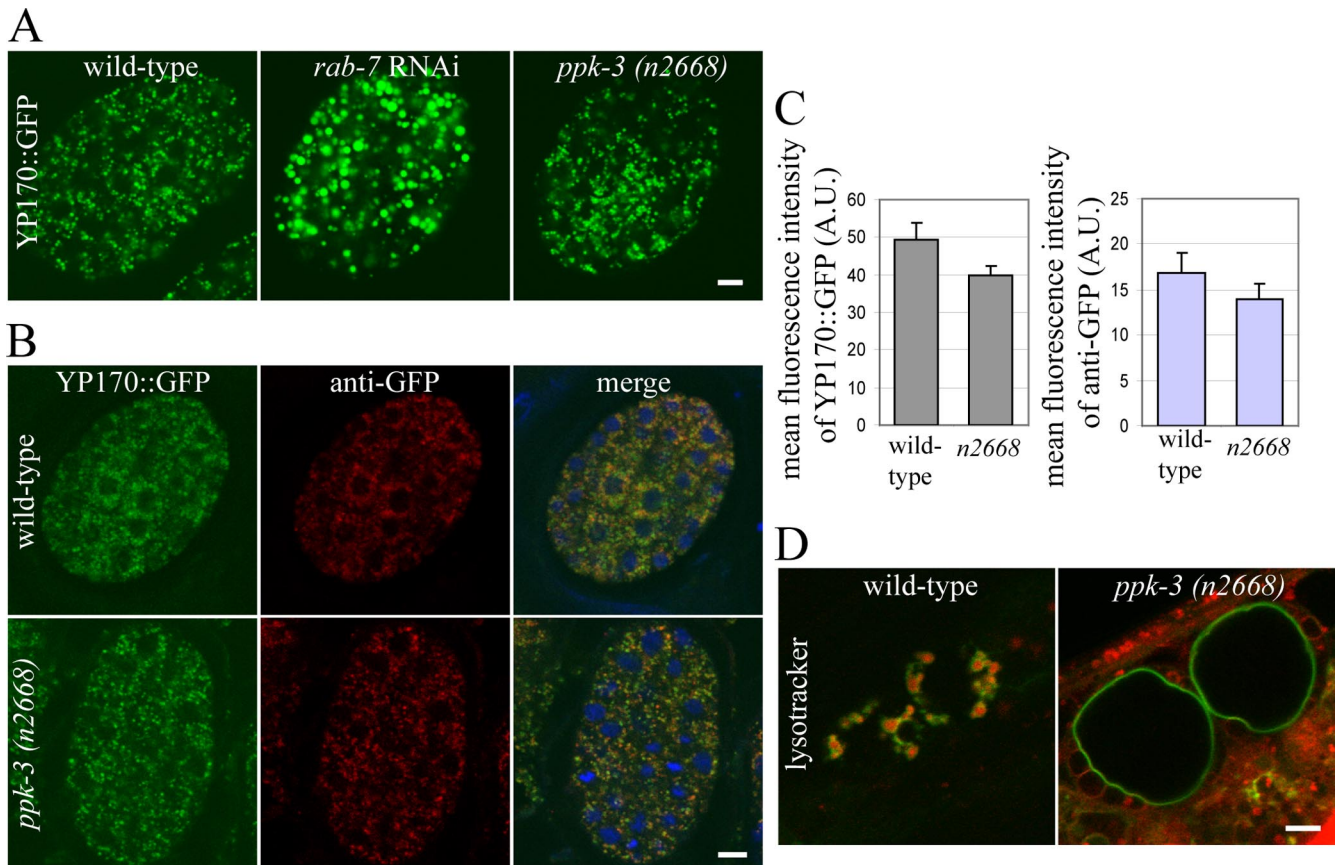


**Figure 8.** Acidification and degradation assays. (A) Confocal pictures of wild-type, *rab-7* (RNAi), and *ppk-3(n2668)* eggs expressing transgenic YP170::GFP (Yolk Protein 170). Bar, 5  $\mu$ m. (B) Confocal pictures of wild-type and *ppk-3(n2668)* eggs expressing transgenic YP170::GFP. The middle panel shows the corresponding anti-GFP labeling (red, Cy3) to rule out possible bleaching of YP170::GFP. The merge picture is shown with nuclear DAPI staining (blue). Bar, 5  $\mu$ m. (C) Quantification of the intensity of YP170::GFP fluorescence from the whole section of embryos on the left and of the anti-GFP antibody signals on the same embryos on the right. A.U., arbitrary unit. (D) Confocal pictures of wild-type and *ppk-3(n2668)* transgenic worms expressing LMP-1::GFP, injected with LysoTracker Red DND-99 (in red), and observed after 5 h. Bar, 5  $\mu$ m.

occurs in *ppk-3* mutants, probably before the enlargement of the lysosomes and neutralization of pH.

#### Defect of PtdIns(3,5)P<sub>2</sub> Production in *ppk-3* Mutants

We monitored the localization of PtdIns(3)P and PtdIns(3,5)P<sub>2</sub>, substrate and product of the PIKfyve/Fab1p kinase activity, respectively, in the *ppk-3(n2668)* mutant, which has a S1356F missense in the catalytic loop. PtdIns(3)P was specifically detected with a probe consisting of a tandem repeat of human HRS FYVE domain (Gillooly *et al.*, 2000; Dang *et al.*, 2004) under the control of a coelomocyte promoter. The limiting membrane of the enlarged lysosome was not labeled for the majority of the coelomocytes, although other vesicles were positive for this probe; one-third of the coelomocytes contain an abnormal vacuole faintly positive for the 2XFYVE probe (Figure 9A). PtdIns(3,5)P<sub>2</sub> was detected with a specific mouse monoclonal antibody in embryos and occurred as cytoplasmic dots. The number of dot-like structures in *ppk-3(n2668)* embryos was highly significantly decreased compared with wild-type ( $p = 2 \times 10^{-7}$ ) (Figure 9, B and C). The remaining PtdIns(3,5)P<sub>2</sub> staining in the mutant might be due either to nonspecific labeling, or to residual production of PtdIns(3,5)P<sub>2</sub> by the mutated PPK-3 or synthesis by an uncharacterized pathway.

To confirm a decrease in PtdIns(3,5)P<sub>2</sub> production, we set up a protocol to measure its level in *C. elegans* by <sup>32</sup>P<sub>i</sub> labeling, separation of [<sup>32</sup>P]phospholipids by thin layer chromatography (TLC) and quantification of the amount of the different isomers of PtdInsP<sub>2</sub> by HPLC. We report for the first time the detection of PtdIns(3,5)P<sub>2</sub> in *C. elegans* where it is present at low level, as it is in yeast and mammalian cells (Dove *et al.*, 1997; Sbrissa *et al.*, 2001). Although *ppk-3* mutants consistently incorporated more <sup>32</sup>P in phospholipids than wild-type worms, we reproducibly observed that the mutants had a much lower level of PtdIns(3,5)P<sub>2</sub> (Figure 9D). We normalized the level of PtdIns(3,5)P<sub>2</sub> on PtdIns(4,5)P<sub>2</sub> and calculated in the representative experiment Figure 9D that PtdIns(3,5)P<sub>2</sub> on PtdIns(4,5)P<sub>2</sub> ratio was 1/40 when comparing *ppk-3* mutant and wild type. Thus, the enlargement of lysosomes seems to be linked to a defect in PtdIns(3,5)P<sub>2</sub> production.

#### DISCUSSION

We have characterized mutants for *ppk-3*, the orthologue of PIKfyve/Fab1p phosphoinositides kinase, in a multicellular organism, *C. elegans*. Mutants show developmental defects: embryonic lethality due to a maternal effect in mutants

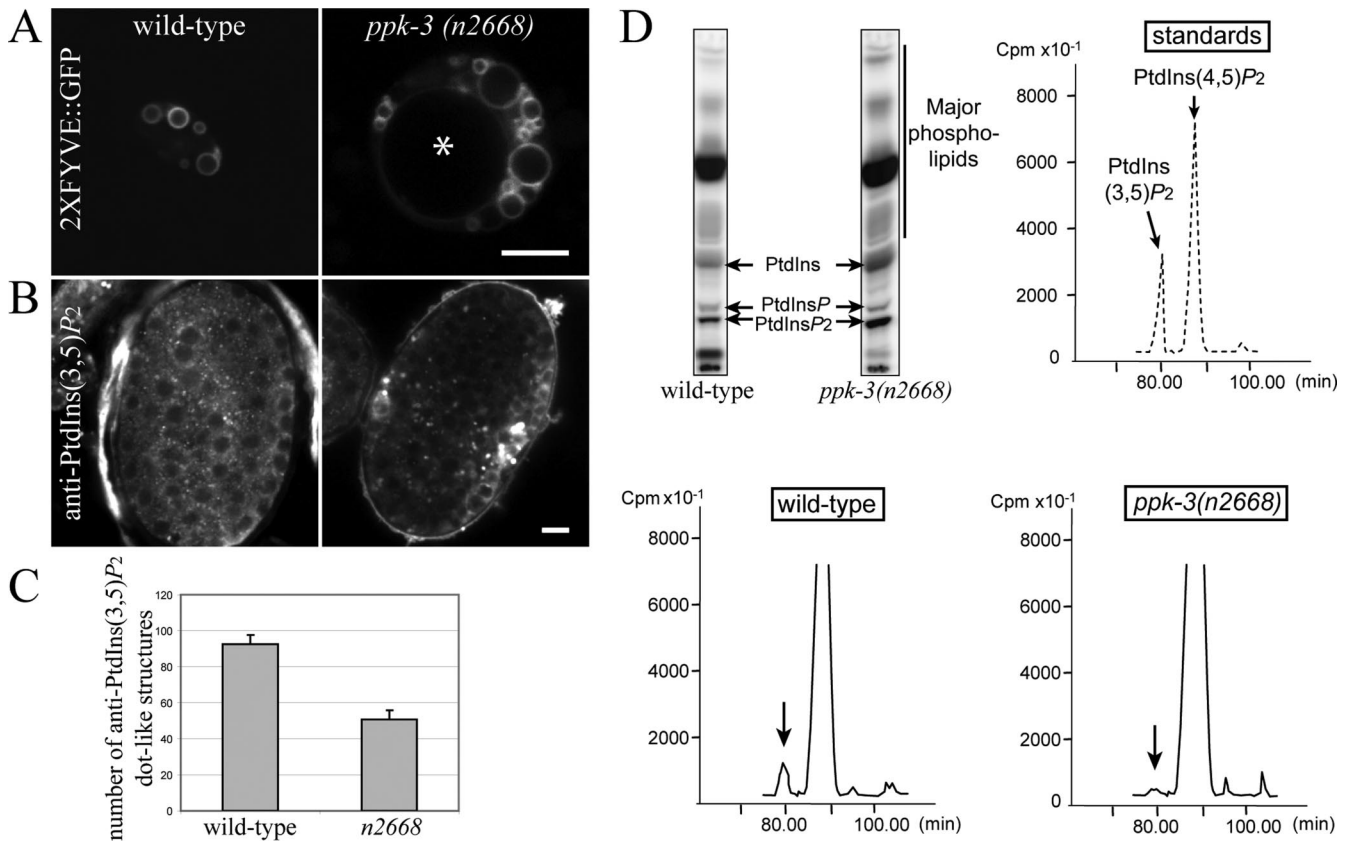


**Figure 9.** PtdIns(3)P and PtdIns(3,5)P<sub>2</sub> localization and level. (A) Confocal picture of wild-type and *ppk-3(n2668)* transgenic worms expressing the 2XFYVE::GFP probe specific of PtdIns(3)P in coelomocytes. The abnormal vacuole of the mutant is indicated by a star. (B) Wild-type and *ppk-3(n2668)* transgenic embryos stained with an anti-PtdIns(3,5)P<sub>2</sub> antibody. Bar, 5  $\mu$ m. (C) Quantification (+SEM) of the number of anti-PtdIns(3,5)P<sub>2</sub> dot-like structures. (D) Lower PtdIns(3,5)P<sub>2</sub> level in the *ppk-3(n2668)* mutant. The worms were labeled with <sup>32</sup>P, lipids were extracted and separated by TLC (left), and the spots corresponding to PtdInsP<sub>2</sub> were analyzed by HPLC (right and bottom). The HPLC profiles illustrating the separation of PtdIns(3,5)P<sub>2</sub> and PtdIns(4,5)P<sub>2</sub> standards as well as the relative level of these two lipids in the different *C. elegans* strains are shown. Arrows on the chromatograms indicate the PtdIns(3,5)P<sub>2</sub>. Data shown are representative of two independent experiments.

carrying a deletion and growth delay in worms with hypomorphic mutations. At the cellular level, we observed a striking enlargement of lysosomes whose membrane originated from smaller lysosomes. Internalization assays and crossing with a *cup-5* mutant defective in lysosome biogenesis showed that the defect is terminal in the maturation of lysosomes. Although these enlarged lysosomes are not acidified, protein degradation is not affected.

We concentrated our studies on the coelomocytes, which are scavenger cells with pronounced endocytosis and degradative functions (Fares and Grant, 2002). In these cells, mutations in *ppk-3* do not have a strong impact on initial uptake and on organelle biogenesis. Studies on mammalian cells transfected with a dominant negative mouse PIKfyve construct (K1831E missense) reported enlargement of MVB-like structures based on electron microscopy (Ikononov *et al.*, 2003a). In contrast, lysosomes seemed nonaffected. In our *ppk-3* mutants, we noted a striking enlargement of the lysosomal compartment, which is more in accordance with the work performed on Fab1p in yeast, where the vacuole compartment is analogous to the lysosome of the higher eukaryotes. Fab1p is implicated in vacuole morphology and homeostasis and is necessary for three different cellular functions (Efe *et al.*, 2005): 1) MVB sorting and protein trans-

port and degradation, 2) vacuole acidification, and 3) membrane recycling from the vacuole. In the *ppk-3* mutant, the fluid phase endocytosis was normal and there was no defect of protein transport to the lysosome and degradation, as monitored with fluorescent proteins transport and GFP and YP170 yolk proteins degradation. Thus, *C. elegans ppk-3* function is not necessary for protein degradation, in coelomocytes. Although the lysosomal enlargement is the most striking, we noted a slight enlargement of RAB-7-positive LMP-1-negative late endosomes in the intestine.

Enlarged lysosomes of the *ppk-3* mutants are not acidic, because they are negative for LysoTracker Red DND-99. This is in accordance with the phenotype described in yeast kinase dead and deleted *Fab1* mutants (Gary *et al.*, 1998). In yeast, the pH of the vacuole is regulated by the V-ATPase proton pump, and in *Fab1* mutants, the transport and assembly of the V-ATPase is not disrupted (Efe *et al.*, 2005). Together, *ppk-3* and *Fab1p* probably regulate directly, or through its PtdIns(3,5)P<sub>2</sub> product, the activity of the V-ATPase. In *C. elegans* coelomocytes, and despite the acidification defect, protein degradation is normal, as shown by GFP uptake and degradation and yolk proteins degradation (Figures 7B and 8). Similarly, Ikononov *et al.* (2003a) noted a normal degradation of the epidermal growth factor recep-

tor in cultured cells overexpressing a dominant negative PIKfyve K1831E mutant (Ikonomov *et al.*, 2003a). Together, *ppk-3* acts mainly on the very late stages of lysosomal maturation, and we hypothesize that degradation occurs before the terminal phenotype of enlargement of lysosomes.

In our mutant, we can distinguish two compartments: early lysosomes that are probably sites of protein degradation, and late lysosomes that are nonacidic and enlarged. Indeed, we have observed fusion between lysosomes and the enlarged vacuoles, which confirm that dynamic exchanges exist between lysosomes, as previously noted in cultured mammalian cells (Deng and Storrie, 1988; Patterson and Lippincott-Schwartz, 2002). In wild-type, we suggest the existence of early and late lysosomes. Degradation occurs in the early acidic lysosomes, and late lysosomes are sites of membrane and protein retrieval. The latter may be nonacidic, a prerequisite for further fusion with other compartments, sustaining the idea that lysosomes are not a dead-end but part of a membrane trafficking cycle in cells (Hirota *et al.*, 2004).

We show that protein degradation and membrane retrieval are uncoupled in the *ppk-3(n2668)* mutant, and we propose that the enlargement of the lysosomes in our *ppk-3* mutant is due to defects in membrane retrieval from matured lysosomes. In yeast, membranes from the vacuole are recycled to the *trans*-Golgi network (Bryant *et al.*, 1998). We have studied coelomocytes, a cell with highly dynamic endocytosis leading to the degradation of protein substrates retrieved from the pseudocoelom. In another cellular context, PPK-3 may play a role on membrane retrieval from other compartments of the endocytic pathway, as in the intestine where there is a slight concomitant enlargement of late endosomes probably due to the fact that there are more membrane retrieval from earlier endosomal compartments to recycle proteins and receptors that should not be degraded. Similarly, PIKfyve could act on membrane retrieval from late endosomes as described in a mammalian cell system (Ikonomov *et al.*, 2002). There, PIKfyve interacts with the Rab9 effector p40 to facilitate membrane trafficking from late endosomes (Ikonomov *et al.*, 2003b). Both regulators of Fab1p, Vac7 and Vac14, were shown to be implicated in membrane retrograde transport (Bonangelino *et al.*, 2002). Atg18, an effector of PtdIns(3,5)P<sub>2</sub>, is implicated in this process and was also implicated in autophagy (Dove *et al.*, 2004; Reggiori *et al.*, 2004). The accumulation of autophagosomes that we observed in the *ppk-3* mutant could reflect a role of PIKfyve in the maturation of autophagosomes and/or in the retrieval of proteins from these compartments. The action of PPK-3 on membrane retrieval is most probably mediated through its product, PtdIns(3,5)P<sub>2</sub>. This is sustained by the observation that the *n2668* hypomorphic *ppk-3* mutant, which has a mutation in the conserved catalytic loop of the kinase domain, shows reduced PtdIns(3,5)P<sub>2</sub> levels compared with wild-type. The phenotypes of this specific mutant should mainly reflect the consequence of the dysregulation of PPK-3 PIs product, PtdIns(3,5)P<sub>2</sub>. Under hyperosmotic shock in yeast, PtdIns(3,5)P<sub>2</sub> is up-regulated and is necessary for the fragmentation of the vacuoles (Bonangelino *et al.*, 2002; LaGrassa and Ungermann, 2005). These data suggest that PtdIns(3,5)P<sub>2</sub> production is required for fission of the lysosome and that its absence in *ppk-3* mutants decreases membrane retrieval, leading to enlargement of this compartment. PtdIns(3,5)P<sub>2</sub> could have a direct role on fission by modifying the physicochemical properties of membranes, by recruiting protein effectors implicated in fission, and/or by regulating retrograde machineries (Carlton *et al.*, 2004).

This study describes for the first time the role of PPK-3 in a multicellular organism. Apart from lysosome morphology, PPK-3 loss has also an impact on the physiology of the worm: we noted an embryonic and larval lethality, and a growth delay. Thus, *ppk-3* has an important role during development and for physiological functions. Interestingly, mutations in human PIKfyve have been recently found in patients with Francois–Neetens Mouchetée fleck corneal dystrophy (OMIM 121850), an autosomal dominant disease (Li *et al.*, 2005). The corneal flecks seem to correspond to keratocytes swollen with poorly characterized enlarged vesicles containing complex lipids and glycosaminoglycans (Nicholson *et al.*, 1977). It is not clear whether the human disease is due to a haplo-insufficiency of PIKfyve function or to a dominant negative effect of the truncated mutations found. Our work suggests that this human disease could be due to a defect in membrane retrieval from late vacuolar compartments. The *ppk-3* mutant worms could be a nice model to study the physiopathology of this disease. PPK-3 and myotubularin phosphatases regulate the level of PtdIns(3,5)P<sub>2</sub>, and some myotubularins are mutated in Charcot–Marie–Tooth neuropathies with anomalies of the myelin sheath (Laporte *et al.*, 2003). The relevance of this PI with respect to myelin formation and stability remains to be determined.

In conclusion, we propose that the enzymatic activity of PPK-3 mainly controls membrane retrieval and not protein degradation. *ppk-3* mutants would be valuable tools to identify new regulators of membrane trafficking not present in yeast and to study the poorly understood destiny of lysosomes.

## ACKNOWLEDGMENTS

We thank Jean-Louis Mandel for fruitful discussions and encouragement; Christine Kretz, Satis Sookhareea, and Gaëtan Chicanne for excellent technical assistance; Anne Gansmuller and Marcel Boeglin for help with electron and confocal microscopies; and members of the group for discussion. We also thank Barth Grant, Beth Levine, Yuji Kohara, and Marc Vidal for providing strains and cDNA clones. Some nematode strains used in this work were provided by the Caenorhabditis Genetics Center, which is funded by the National Institutes of Health National Center for Research Resources. A.D.C. acknowledges the support of H. R. Horvitz, in whose laboratory the *n2668* and *n2835* mutations were isolated. This work was supported by the Institut National de la Santé et de la Recherche Médicale, the Centre National de la Recherche Scientifique, the Collège de France, and the Association Française contre les Myopathies. H. F. is supported by National Institute of General Medical Sciences Grant GM-65235. A.D.C. is supported by National Institutes of Health Grant GM-54657. A.-S.N. is recipient of a Bourse de Docteur Ingénieur (Centre National de la Recherche Scientifique-Région Alsace) fellowship.

## REFERENCES

- Azzedine, H., *et al.* (2003). Mutations in MTMR13, a new pseudophosphatase homologue of MTMR2 and Sbf1, in two families with an autosomal recessive demyelinating form of Charcot-Marie-Tooth disease associated with early-onset glaucoma. *Am. J. Hum. Genet.* 72, 1141–1153.
- Bargal, R., Avidan, N., Ben-Asher, E., Olender, Z., Zeigler, M., Frumkin, A., Raas-Rothschild, A., Glusman, G., Lancet, D., and Bach, G. (2000). Identification of the gene causing mucopolipidosis type IV. *Nat. Genet.* 26, 118–123.
- Berwick, D. C., Dell, G. C., Welsh, G. I., Heesom, K. J., Hers, I., Fletcher, L. M., Cooke, F. T., and Tavare, J. M. (2004). Protein kinase B phosphorylation of PIKfyve regulates the trafficking of GLUT4 vesicles. *J. Cell Sci.* 117, 5985–5993.
- Bligh, E. G., and Dyer, W. J. (1959). A rapid method of total lipid extraction and purification. *Can. J. Biochem. Physiol.* 37, 911–917.
- Bolino, A., *et al.* (2000). Charcot-Marie-Tooth type 4B is caused by mutations in the gene encoding myotubularin-related protein-2. *Nat. Genet.* 25, 17–19.
- Bonangelino, C. J., Nau, J. J., Duex, J. E., Brinkman, M., Wurmser, A. E., Gary, J. D., Emr, S. D., and Weisman, L. S. (2002). Osmotic stress-induced increase of phosphatidylinositol 3,5-bisphosphate requires Vac14p, an activator of the lipid kinase Fab1p. *J. Cell Biol.* 156, 1015–1028.

- Brenner, S. (1974). The genetics of *Caenorhabditis elegans*. *Genetics* 77, 74–94.
- Bright, N. A., Gratian, M. J., and Luzio, J. P. (2005). Endocytic delivery to lysosomes mediated by concurrent fusion and kissing events in living cells. *Curr. Biol.* 15, 360–365.
- Britton, C., and Murray, L. (2004). Cathepsin L protease (CPL-1) is essential for yolk processing during embryogenesis in *Caenorhabditis elegans*. *J. Cell Sci.* 117, 5133–5143.
- Bryant, N. J., Piper, R. C., Weisman, L. S., and Stevens, T. H. (1998). Retrograde traffic out of the yeast vacuole to the TGN occurs via the prevacuolar/endosomal compartment. *J. Cell Biol.* 142, 651–663.
- Burda, P., Padilla, S. M., Sarkar, S., and Emr, S. D. (2002). Retromer function in endosome-to-Golgi retrograde transport is regulated by the yeast Vps34 PtdIns 3-kinase. *J. Cell Sci.* 115, 3889–3900.
- Carlton, J., Bujny, M., Peter, B. J., Oorschot, V. M., Rutherford, A., Mellor, H., Klumperman, J., McMahon, H. T., and Cullen, P. J. (2004). Sorting nexin-1 mediates tubular endosome-to-TGN transport through coincidence sensing of high-curvature membranes and 3-phosphoinositides. *Curr. Biol.* 14, 1791–1800.
- Chen, C. C., Schweinsberg, P. J., Vashist, S., Mareiniss, D. P., Lambie, E. J., and Grant, B. D. (2006). RAB-10 is required for endocytic recycling in the *Caenorhabditis elegans* intestine. *Mol. Biol. Cell* 17, 1286–1297.
- Clokey, G. V., and Jacobson, L. A. (1986). The autofluorescent “lipofuscin granules” in the intestinal cells of *Caenorhabditis elegans* are secondary lysosomes. *Mech. Ageing Dev.* 35, 79–94.
- Dang, H., Li, Z., Skolnik, E. Y., and Fares, H. (2004). Disease-related myotubularin function in endocytic traffic in *Caenorhabditis elegans*. *Mol. Biol. Cell* 15, 189–196.
- Deng, Y. P., and Storrie, B. (1988). Animal cell lysosomes rapidly exchange membrane proteins. *Proc. Natl. Acad. Sci. USA* 85, 3860–3864.
- Dove, S. K., Cooke, F. T., Douglas, M. R., Sayers, L. G., Parker, P. J., and Michell, R. H. (1997). Osmotic stress activates phosphatidylinositol-3,5-bisphosphate synthesis. *Nature* 390, 187–192.
- Dove, S. K., et al. (2004). Svp1p defines a family of phosphatidylinositol 3,5-bisphosphate effectors. *EMBO J.* 23, 1922–1933.
- Efe, J. A., Botelho, R. J., and Emr, S. D. (2005). The Fab1 phosphatidylinositol kinase pathway in the regulation of vacuole morphology. *Curr. Opin. Cell Biol.* 17, 402–408.
- Fares, H., and Grant, B. (2002). Deciphering endocytosis in *Caenorhabditis elegans*. *Traffic* 3, 11–19.
- Fares, H., and Greenwald, I. (2001). Regulation of endocytosis by CUP-5, the *Caenorhabditis elegans* mucolipin-1 homolog. *Nat. Genet.* 28, 64–68.
- Friant, S., Pecheur, E. I., Eugster, A., Michel, F., Lefkir, Y., Nourrisson, D., and Letourneur, F. (2003). Ent3p Is a PtdIns(3,5)P2 effector required for protein sorting to the multivesicular body. *Dev. Cell* 5, 499–511.
- Gary, J. D., Wurmser, A. E., Bonangelino, C. J., Weisman, L. S., and Emr, S. D. (1998). Fab1p is essential for PtdIns(3)P 5-kinase activity and the maintenance of vacuolar size and membrane homeostasis. *J. Cell Biol.* 143, 65–79.
- Gillooly, D. J., Morrow, I. C., Lindsay, M., Gould, R., Bryant, N. J., Gaullier, J. M., Parton, R. G., and Stenmark, H. (2000). Localization of phosphatidylinositol 3-phosphate in yeast and mammalian cells. *EMBO J.* 19, 4577–4588.
- Grant, B., and Hirsh, D. (1999). Receptor-mediated endocytosis in the *Caenorhabditis elegans* oocyte. *Mol. Biol. Cell* 10, 4311–4326.
- Griffin, C. T., Trejo, J., and Magnuson, T. (2005). Genetic evidence for a mammalian retromer complex containing sorting nexins 1 and 2. *Proc. Natl. Acad. Sci. USA* 102, 15173–15177.
- Gruenberg, J., and Stenmark, H. (2004). The biogenesis of multivesicular endosomes. *Nat. Rev. Mol. Cell Biol.* 5, 317–323.
- Hirota, Y., Masuyama, N., Kuronita, T., Fujita, H., Himeno, M., and Tanaka, Y. (2004). Analysis of post-lysosomal compartments. *Biochem. Biophys. Res. Commun.* 314, 306–312.
- Ikonomov, O. C., Sbrissa, D., Foti, M., Carpentier, J. L., and Shisheva, A. (2003a). PIKfyve controls fluid phase endocytosis but not recycling/degradation of endocytosed receptors or sorting of procathepsin D by regulating multivesicular body morphogenesis. *Mol. Biol. Cell* 14, 4581–4591.
- Ikonomov, O. C., Sbrissa, D., Mlak, K., Deeb, R., Fligger, J., Soans, A., Finley, R. L., Jr., and Shisheva, A. (2003b). Active PIKfyve associates with and promotes the membrane attachment of the late endosome-to-*trans*-Golgi network transport factor Rab9 effector p40. *J. Biol. Chem.* 278, 50863–50871.
- Ikonomov, O. C., Sbrissa, D., Mlak, K., Kanzaki, M., Pessin, J., and Shisheva, A. (2002). Functional dissection of lipid and protein kinase signals of PIKfyve reveals the role of PtdIns 3,5-P2 production for endomembrane integrity. *J. Biol. Chem.* 277, 9206–9211.
- Kostich, M., Fire, A., and Fambrough, D. M. (2000). Identification and molecular-genetic characterization of a LAMP/CD68-like protein from *Caenorhabditis elegans*. *J. Cell Sci.* 113, 2595–2606.
- LaGrassa, T. J., and Ungermann, C. (2005). The vacuolar kinase Yck3 maintains organelle fragmentation by regulating the HOPS tethering complex. *J. Cell Biol.* 168, 401–414.
- Laporte, J., Bedez, F., Bolino, A., and Mandel, J.-L. (2003). Cooperation and specificity of catalytically active and inactive myotubularin phosphoinositides phosphatases. *Hum. Mol. Genet.* 12, 285–292.
- Laporte, J., Hu, L. J., Kretz, C., Mandel, J. L., Kioschis, P., Coy, J. F., Klauck, S. M., Poustka, A., and Dahl, N. (1996). A gene mutated in X-linked myotubular myopathy defines a new putative tyrosine phosphatase family conserved in yeast. *Nat. Genet.* 13, 175–182.
- Li, S., et al. (2005). Mutations in PIP5K3 Are Associated with Francois-Neetens Mouchette Fleck Corneal Dystrophy. *Am. J. Hum. Genet.* 77, 54–63.
- McIntire, S. L., Garriga, G., White, J., Jacobson, D., and Horvitz, H. R. (1992). Genes necessary for directed axonal elongation or fasciculation in *C. elegans*. *Neuron* 8, 307–322.
- McKay, S. J., et al. (2003). Gene expression profiling of cells, tissues, and developmental stages of the nematode *C. elegans*. *Cold Spring Harb. Symp. Quant. Biol.* 68, 159–169.
- Melendez, A., Tallozy, Z., Seaman, M., Eskelinen, E. L., Hall, D. H., and Levine, B. (2003). Autophagy genes are essential for dauer development and life-span extension in *C. elegans*. *Science* 301, 1387–1391.
- Miaczynska, M., Pelkmans, L., and Zerial, M. (2004). Not just a sink: endosomes in control of signal transduction. *Curr. Opin. Cell Biol.* 16, 400–406.
- Michaux, G., Gansmuller, A., Hindelang, C., and Labouesse, M. (2000). CHE-14, a protein with a sterol-sensing domain, is required for apical sorting in *C. elegans* ectodermal epithelial cells. *Curr. Biol.* 10, 1098–1107.
- Nicholson, D. H., Green, W. R., Cross, H. E., Kenyon, K. R., and Massof, D. (1977). A clinical and histopathological study of Francois-Neetens speckled corneal dystrophy. *Am. J. Ophthalmol.* 83, 554–560.
- Odorizzi, G., Babst, M., and Emr, S. D. (1998). Fab1p PtdIns(3)P 5-kinase function essential for protein sorting in the multivesicular body. *Cell* 95, 847–858.
- Patterson, G. H., and Lippincott-Schwartz, J. (2002). A photoactivatable GFP for selective photolabeling of proteins and cells. *Science* 297, 1873–1877.
- Patton, A., Knuth, S., Schaheen, B., Dang, H., Greenwald, I., and Fares, H. (2005). Endocytosis function of a ligand-gated ion channel homolog in *Caenorhabditis elegans*. *Curr. Biol.* 15, 1045–1050.
- Payrastra, B. (2004). Phosphoinositides: lipid kinases and phosphatases. *Methods Mol. Biol.* 273, 201–212.
- Reggiori, F., Tucker, K. A., Stromhaug, P. E., and Klionsky, D. J. (2004). The Atg1-Atg13 complex regulates Atg9 and Atg23 retrieval transport from the pre-autophagosomal structure. *Dev. Cell* 6, 79–90.
- Rink, J., Ghigo, E., Kalaidzidis, Y., and Zerial, M. (2005). Rab conversion as a mechanism of progression from early to late endosomes. *Cell* 122, 735–749.
- Sbrissa, D., Ikonomov, O., and Shisheva, A. (2001). Selective insulin-induced activation of class I(A) phosphoinositide 3-kinase in PIKfyve immune complexes from 3T3-L1 adipocytes. *Mol. Cell Endocrinol.* 181, 35–46.
- Schultz, J., Copley, R. R., Doerks, T., Ponting, C. P., and Bork, P. (2000). SMART: a Web-based tool for the study of genetically mobile domains. *Nucleic Acids Res.* 28, 231–234.
- Seaman, M. N. (2005). Recycle your receptors with retromer. *Trends Cell Biol.* 15, 68–75.
- Senderek, J., Bergmann, C., Weber, S., Ketelsen, U. P., Schorle, H., Rudnik-Schoneborn, S., Buttner, R., Buchheim, E., and Zerres, K. (2003). Mutation of the SBF2 gene, encoding a novel member of the myotubularin family, in Charcot-Marie-Tooth neuropathy type 4B2/11p15. *Hum. Mol. Genet.* 12, 349–356.
- Shisheva, A. (2001). PIKfyve: the road to PtdIns 5-P and PtdIns 3,5-P(2). *Cell Biol. Int.* 25, 1201–1206.
- Simonsen, A., Wurmser, A. E., Emr, S. D., and Stenmark, H. (2001). The role of phosphoinositides in membrane transport. *Curr. Opin. Cell Biol.* 13, 485–492.
- Thompson, J. D., Gibson, T. J., Plewniak, F., Jeanmougin, F., and Higgins, D. G. (1997). The CLUSTAL\_X windows interface: flexible strategies for multiple sequence alignment aided by quality analysis tools. *Nucleic Acids Res.* 25, 4876–4882.

- Timmons, L., and Fire, A. (1998). Specific interference by ingested dsRNA. *Nature* 395, 854.
- Treusch, S., Knuth, S., Slaugenhaupt, S. A., Goldin, E., Grant, B. D., and Fares, H. (2004). *Caenorhabditis elegans* functional orthologue of human protein h-mucopolipin-1 is required for lysosome biogenesis. *Proc. Natl. Acad. Sci. USA* 101, 4483–4488.
- Wei, A., Yuan, A., Fawcett, G., Butler, A., Davis, T., Xu, S. Y., and Salkoff, L. (2002). Efficient isolation of targeted *Caenorhabditis elegans* deletion strains using highly thermostable restriction endonucleases and PCR. *Nucleic Acids Res.* 30, e110.
- Wenk, M. R., and De Camilli, P. (2004). Protein-lipid interactions and phosphoinositide metabolism in membrane traffic: insights from vesicle recycling in nerve terminals. *Proc. Natl. Acad. Sci. USA* 101, 8262–8269.
- Whitley, P., Reaves, B. J., Hashimoto, M., Riley, A. M., Potter, B. V., and Holman, G. D. (2003). Identification of mammalian Vps24p as an effector of phosphatidylinositol 3,5-bisphosphate-dependent endosome compartmentalization. *J. Biol. Chem.* 278, 38786–38795.
- Zhang, Y., Grant, B., and Hirsh, D. (2001). RME-8, a conserved J-domain protein, is required for endocytosis in *Caenorhabditis elegans*. *Mol. Biol. Cell* 12, 2011–2021.